Supplement of Geosci. Model Dev., 14, 661–674, 2021
https://doi.org/10.5194/gmd-14-661-2021-supplement

Geoscientific Model Development
Open Access
EGU

Supplement of

Methane chemistry in a nutshell – the new submodels CH4 (v1.0) and TRSYNC (v1.0) in MESSy (v2.54.0)

Franziska Winterstein and Patrick Jöckel

Correspondence to: Franziska Winterstein (franziska.winterstein@dlr.de)

Contents

S1 Chemical processes and reaction rate coefficients concerning CH_4

S1.1 Sink reactions

General sink reactions:

$$CH_4 + OH \overset{k_{CH_4+OH}}{\rightarrow} CH_3 + H_2O \quad \text{(SR1)}$$

$$CH_4 + O(^1D) \overset{k_{CH_4+O(^1D)}}{\rightarrow} products \quad \text{(SR2)}$$

$$CH_4 + Cl \overset{k_{CH_4+Cl}}{\rightarrow} CH_3 + HCl \quad \text{(SR3)}$$

$$CH_4 + h\nu \overset{k_{CH_4+h\nu}}{\rightarrow} products \quad \text{(SR4)}$$

Sink reactions with isotopologues containing carbon-13 (^{13}C) :

$$^{13}CH_4 + OH \overset{k_{^{13}CH_4+OH}}{\rightarrow} {}^{13}CH_3 + H_2O \quad \text{(SR5)}$$

$$^{13}CH_4 + O(^1D) \overset{k_{^{13}CH_4+O(^1D)}}{\rightarrow} products \quad \text{(SR6)}$$

$$^{13}CH_4 + Cl \overset{k_{^{13}CH_4+Cl}}{\rightarrow} {}^{13}CH_3 + HCl \quad \text{(SR7)}$$

$$^{13}CH_4 + h\nu \overset{k_{^{13}CH_4+h\nu}}{\rightarrow} products \quad \text{(SR8)}$$

Sink reactions with isotopologues containing deuterium (D):

$$CH_3D + OH \overset{k_{CH_3D+OH}}{\rightarrow} CH_2D + H_2O \quad \text{(SR9)}$$

$$CH_3 + HDO \quad \text{(SR10)}$$

$$CH_3D + O(^1D) \overset{k_{CH_3D+O(^1D)}}{\rightarrow} products \quad \text{(SR11)}$$

$$CH_3D + Cl \overset{k_{CH_3D+Cl}}{\rightarrow} CH_2D + HCl \quad \text{(SR12)}$$

$$CH_3 + DCl \quad \text{(SR13)}$$

$$CH_3D + h\nu \overset{k_{CH_3D+h\nu}}{\rightarrow} products \quad \text{(SR14)}$$

S1.2 Reaction rate coefficients

The reaction rates for the reaction (SR1–SR3) applied in this study are:

$$k_{CH_4+OH} = 1.85 \times 10^{-20} \cdot \exp(2.82 \cdot \log(T) - \frac{987}{T}) \quad (1)$$

$$= 1.85 \times 10^{-20} \cdot T^{2.82} \cdot \exp(-\frac{987}{T}) \quad (2)$$

$$k_{CH_4+Cl} = 6.6 \times 10^{-12} \cdot \exp(\frac{-1240}{T}) \quad (3)$$

$$k_{CH_4+O1D} = 1.75 \times 10^{-10} \quad (4)$$

Eq. (3) and (4) are from Sander et al. (2011) and Eq. (1) from Atkinson (2003). The temperature in [K] is denoted as T.

The reaction rate coefficients for the isotopologues (SR5–SR14) are achieved by multiplying the inverse of the corresponding kinetic isotope effect (KIE) from Table 1 in the main manuscript. For example:

$$k_{^{13}CH_4+OH} = k_{CH_4+OH} \cdot \mathrm{KIE}^{\mathrm{OH}-1}_{^{13}CH_4} \quad (5)$$

Table S1. The isotopic signature of the emission sources as used in the model simulations with ECHAM/MESSy Atmospheric Chemistry (EMAC). All δ-values and ranges are given in [permil (‰)].

	δ^{13}C(CH_4)$_{VPDB}$			δD(CH_4)$_{VSMOW}$		
Natural sources	δ-value	$\pm$	references	δ-value	$\pm$	references
wetlands	-59.4	1.5	[1,2,3,4,6]	-336.2	23.8	[3,4,6]
other						
wildanimals	-61.5	0.5	[1]	-319.0	/	[5]
termites	-63.3	6.5	[1,2,3]	-390.0	35.5	[3]
volcanoes	-40.9	0.9	[1,2]	-253.4	53.4	[3,7]
ocean (hydrates)	-59.0	1.0	[1,2,3]	-220.0	/	[3]
Anthropogenic sources						
anthropogenic (collective)	-46.8	10.3	[3,4,6,8]	-223.5	23.5	[3,4,6]
rice	-63.0	1.0	[1,2,3,4,6]	-324.3	5.5	[3,4,6]
biomass burning	-23.9	1.6	[1,2,3,4,6]	-213.0	7.5	[3,4,6]

references: (1) (Monteil et al., 2011) (2) (Fletcher et al., 2004) (3) (Whiticar and Schaefer, 2007) (4) (Snover and Quay, 2000) (5) (Rigby et al., 2012) (6) (Quay et al., 1999) (7) (Kiyosu, 1983) (8) (Zazzeri et al., 2015)

S2 Evaluation of simulated CH_4 isotopologues with observations

The following section shows comparisons of simulation results with atmospheric observations from stationary surface sampling sites of the National Oceanic and Atmospheric Administration/Earth System Research Laboratory (NOAA/ESRL, White et al. (2016, 2017)), with airborne observations taken during the Comprehensive Observation Network for TRace gases by AIrLiner (CONTRAIL) project (Umezawa et al., 2012), and with balloon borne observations by Röckmann et al. (2011). The study is based on work by Frank (2018) and observations are thereby compared to two simulations (1) EMAC-apos-02 and (2) EMAC-apos-03.

In the simulation EMAC-apos-02, the CH4 submodel together with its isotopologue extension is applied. This includes isotopologues concerning both, carbon, and hydrogen isotopes. The submodel is set up with the KIEs as introduced in Table 1 (see main manuscript). The comprehensive interactive chemistry simulation EMAC-apos-03 is conducted with the kinetic chemistry tagging technique (MECCA_TAG) concerning hydrogen isotopologues, only. This configuration is chosen to investigate the pathways of deuterium from the source towards the end-product of deuterated methane (CH_3D), i.e. deuterated water vapour (HDO). This requires to include KIEs for the intermediates, too, as well as to apply adequate branching ratios and isotope transfer probabilities. The inclusion of carbon isotopologues with MECCA_TAG is omitted due to the fact that MECCA_TAG introduces additionally nearly twice as many chemical reactions and species as included in the basic chemical mechanism. To maintain a computational efficient simulation, the CH4 submodel is in EMAC-apos-03 additionally applied to simulate the carbon related methane (CH_4) isotopologues. In this case, the CH_4 tracer of the simplified CH_4 chemistry (CH4) submodel (`CH4_fx`), acting as the master tracer for the CH_4 isotopologues in the CH4 submodel, is in each model time step reset to the CH_4 tracer in the Module Efficiently Calculating the Chemistry of the Atmosphere (MECCA) to ensure an identical overall CH_4 budget. The CH4 submodel also uses directly the on-line calculated the hydroxyl radical (OH), excited oxygen ($O(^1D)$) and chlorine (Cl) distribution from MECCA.

The applied emission inventory in the presented simulations is an a posteriori inventory derived using an inverse optimization technique (Frank, 2018; Bruhwiler et al., 2005). The specific isotopic signatures of the emission sources used in the model are listed in Table S1.

The isotopic signatures are given in the δ-notation (McKinney et al., 1950). We use the standard isotopic signature of Vienna Standard Mean Ocean Water (VSMOW) for the signature of D in CH_4 (δD(CH_4)) and Vienna PeeDee Belemnite (VPDB) for the signature of ^{13}C in CH_4 (δ^{13}C(CH_4)).

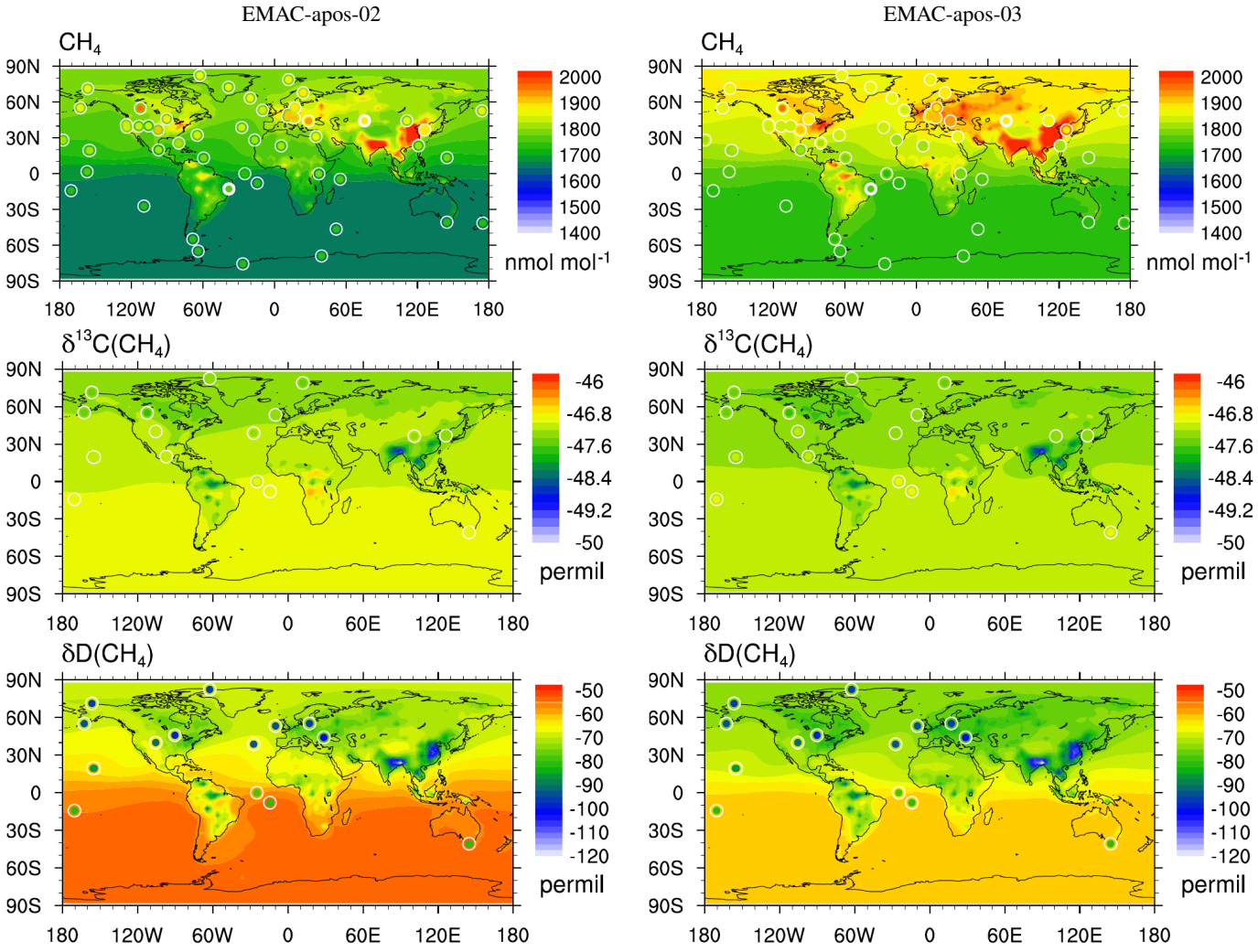

Figure S1. Simulated multi-annual (2000–2009) surface mixing ratio of CH_4 in [nmoles of the chemical tracer per mole of air (mol mol^{-1})] (upper), corresponding $\delta^{13}C(CH_4)_{VPDB}$ in [‰] (middle), and $\delta D(CH_4)_{VSMOW}$ in [‰] (lower). The left column shows results of EMAC-apos-02 and the right column those from EMAC-apos-03. The colored dots indicate the surface observations from NOAA/ESRL. The circles around the dots are the value of the simulation at the specific sampling height of the observation (in order to account for sub-grid orographic differences between simulation and observation).

S2.1 Surface sampling sites

To start with the evaluation of the simulation results, isotopic observations from NOAA/ESRL sampling sites (White et al., 2016, 2017) are compared to the surface mixing ratios and δ-values of the simulations. For the comparison a climatological mean of 2000–2009 is used, since this time period is represented by most of the stations and the dynamic equilibrium of the simulated isotopic composition (as visible especially in EMAC-apos-03, Frank (2018)) has been reached.

EMAC-apos-03 agrees well with the stations regarding the CH_4 mixing ratio. Interesting is that the $\delta^{13}C(CH_4)$ values are slightly better represented in EMAC-apos-02 compared to EMAC-apos-03, although the agreement is overall quite well in both simulations. This suggests that the emission signatures are a bit too low for methane containing ^{13}C ($^{13}CH_4$) in connection

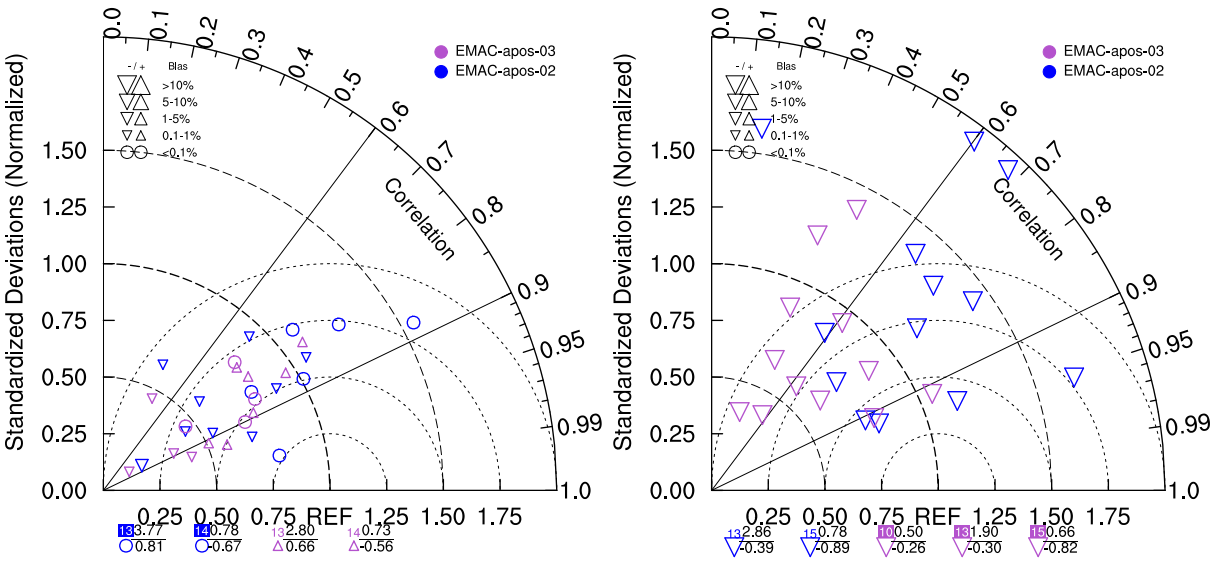

Figure S2. Taylor diagrams of the comparison between observations and the simulations EMAC-apos-02 (blue) and EMAC-apos-03 (purple) at various surface sampling sites. The Taylor diagram is shown for $\delta^{13}C(CH_4)_{VPDB}$ (a) and for $\delta D(CH_4)_{VSMOW}$ (b) with respect to the representation of the annual cycle during the considered time period 2000–2009. The size of the triangles indicates the bias in percent with upward oriented triangles indicating a positive and downward oriented triangles a negative bias, respectively. Circles indicate a bias of less than 0.1%. The symbols below the diagram are stations outside the displayed range of the Taylor diagram and are indicated by the colored number. The normalized standard deviation is displayed by the upper black number and the correlation coefficient by the lower black number on the right hand side of the symbol.

with the OH concentration in EMAC-apos-03. On the other hand, in case of $\delta D(CH_4)$, EMAC-apos-03 agrees better, however, is still isotopically enriched compared to the station samples. This indicates that the chosen emission signatures for CH_3D are too heavy.

In addition to that, the annual cycle of the observations is generally fairly well represented in both simulations (see Fig. S2). However, the trend of the signatures at the stations over the years could not be captured yet. The reason for this is that the simulations fail to represent the general trend of the CH_4 mixing ratio and that the emission signatures of the individual sources are still uncertain.

S2.2 Airborne observations

During the CONTRAIL project, atmospheric air samples were taken with an Automatic air Sampling Equipment (ASE) mounted on a commercial aircraft (Umezawa et al., 2012). These air samples were later measured concerning the isotopic composition of CH_4 using a gas chromatography system and a flame ionization detector. The here presented sampling data comprise several flights between 2006 and 2010, with each flight providing up to 12 air samples.

The presented flights are seperated into two regions, as depicted in Fig. S3. The first region (green) indicates the flights on a north-south route, bound from Narita airport (Japan) to Sydney, Brisbane (Australia) or Guam, and the second region (red) represents those flights on an east-west route, bound from Narita to Honolulu (Hawaii).

Especially the first region provides the opportunity to investigate the representation of the meridional gradient and the north-south imbalance in the δ-values in the model as it nicely spans over the tropics (40° S-40° N). Simulation results and the airborne observations in this region are depicted in Fig. S4, where green dots indicate the observations. The dark green line

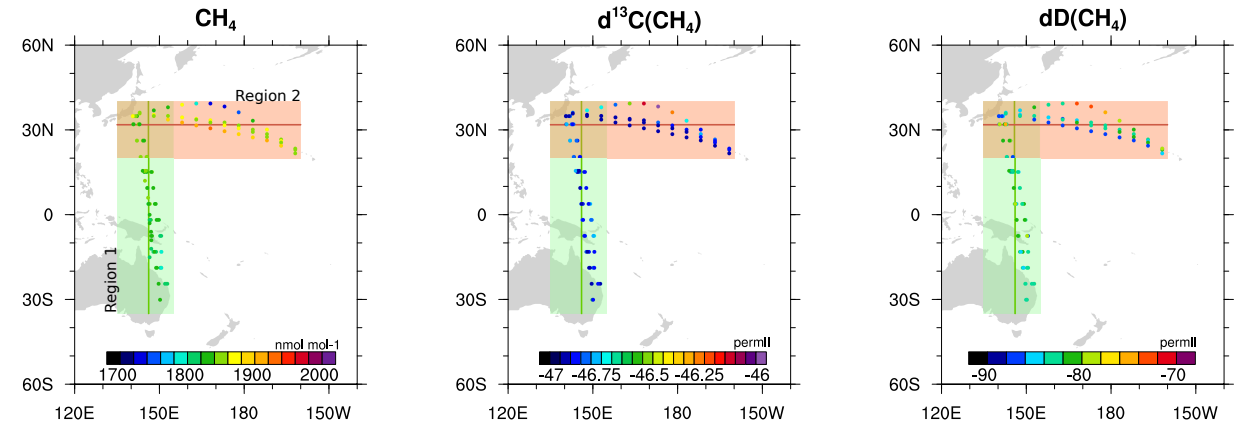

Figure S3. Observations provided by the CONTRAIL project (Umezawa et al., 2012). The green shaded area indicates region 1, and the red shaded area indicates region 2.

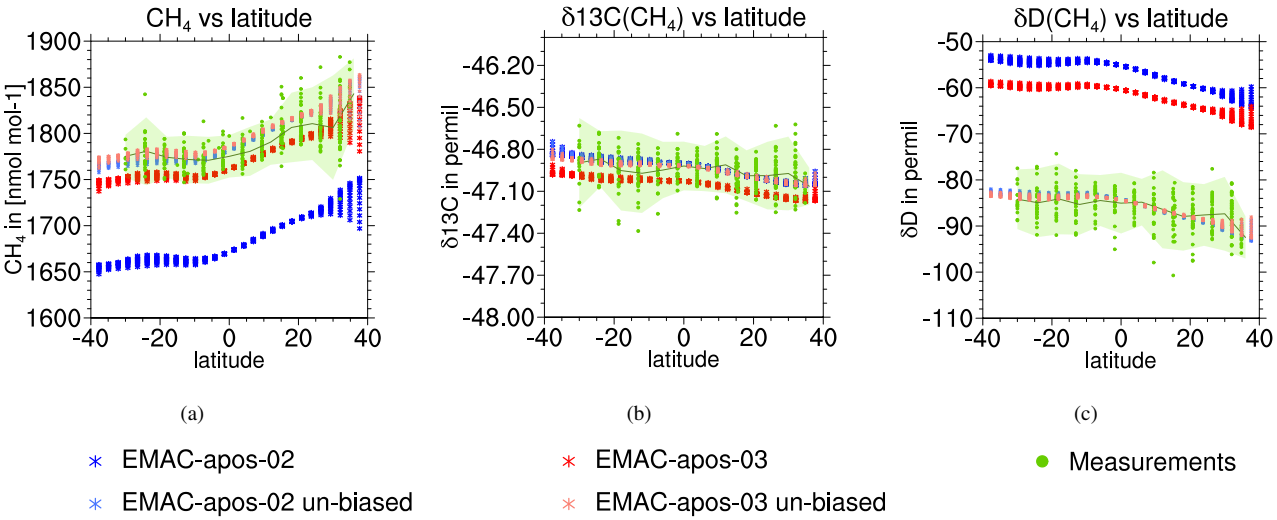

Figure S4. Comparison of airborne observations (green) in the meridionally aligned region 1 with simulation data from EMAC-apos-02 (blue) and EMAC-apos-03 (red). CH_4 (a), $\delta^{13}C(CH_4)_{VPDB}$ (b) and $\delta D(CH_4)_{VSMOW}$ (c). The lighter red and blue colored markers indicate the de-biased simulation data for the direct comparison to the meridional gradient of the observations. The dark green line indicates the mean of the observations with the greenish shaded area being the corresponding single standard deviation.

indicates the mean of the observations and the shaded green area is the corresponding standard deviation. Simulated values are included as the red and blue dots respectively.

It is apparent from the shown results that the meridional gradient in the simulations concerning CH_4 and both isotopic signatures are well represented, although the absolute values differ. This indicates that the implemented KIE in the model is reasonable and that adjustments to the signatures of the emission inventory are required.

S2.3 Balloon borne observations

The presented airborne observations are used to infer tropospheric chemical compositions. The high-altitude range of balloon borne observations enables to investigate the stratospheric isotopic signatures, as well.

The observational data are provided by Röckmann et al. (2011) and were obtained by altogether 13 balloon flights between 1987 and 2003 at four launch stations: Hyderabab in India (HYD), Aire sur l'Adour in France (ASA), Gap in France (GAP) and Kiruna in Sweden (KIR). The balloon-borne high-altitude air samples are obtained up to 10 hPa (35 km) and were later examined with respect to CH_4 mixing ratios as well as its isotopic composition concerning $^{13}CH_4$ and CH_3D using a high precision continuous flow isotope ratio mass spectrometer (Brass and Röckmann, 2010).

The observations shown in Fig. S5 indicate two features:

- First, while CH_4 gets reduced towards higher altitudes, the isotopic content gets enriched (both, in $\delta^{13}C(CH_4)$ and $\delta D(CH_4)$). This occurs due to fractionation processes, which prefer lighter isotopologues in the sink reactions over heavier isotopologues.
- Secondly, again, a meridional gradient is visible. Polar regions tend to have less CH_4 than tropical regions, indicating to some extent the older age of the polar air masses. Consequently, polar regions are isotopically enriched compared to regions at mid and low latitudes.

The balloon-borne observations are compared to the simulations in Fig. S5 at pressure levels from 200 hPa to 10 hPa and separated into polar, mid-latitude and tropical regions. For the comparison, the monthly averaged data of the simulation is sampled at the specific year, month and location of the observation and interpolated from model levels to pressure levels. The plots in Fig. S5 further show the single standard deviation of the observations by the grey shaded areas and the standard deviation of all vertical profiles in the corresponding latitudinal region of the simulations as the shaded area in the color of the respective simulation.

The presented comparisons of observations to simulation results show that the global isotopic features of the meridional isotopic gradient and the isotopic gradient with altitude is captured well by both simulations (EMAC-apos-02, only with CH4 submodel, and EMAC-apos-03, with MECCA and the CH4 submodel). This indicates that the implementation of the simulation of CH_4 isotopologues is sufficiently realized and also confirms the suitability of the chosen KIE values. Absolute values and the inter-annual trend of the observations, however, are not captured well, which is mainly caused by uncertainties in the CH_4 emission fluxes and the applied source signatures.

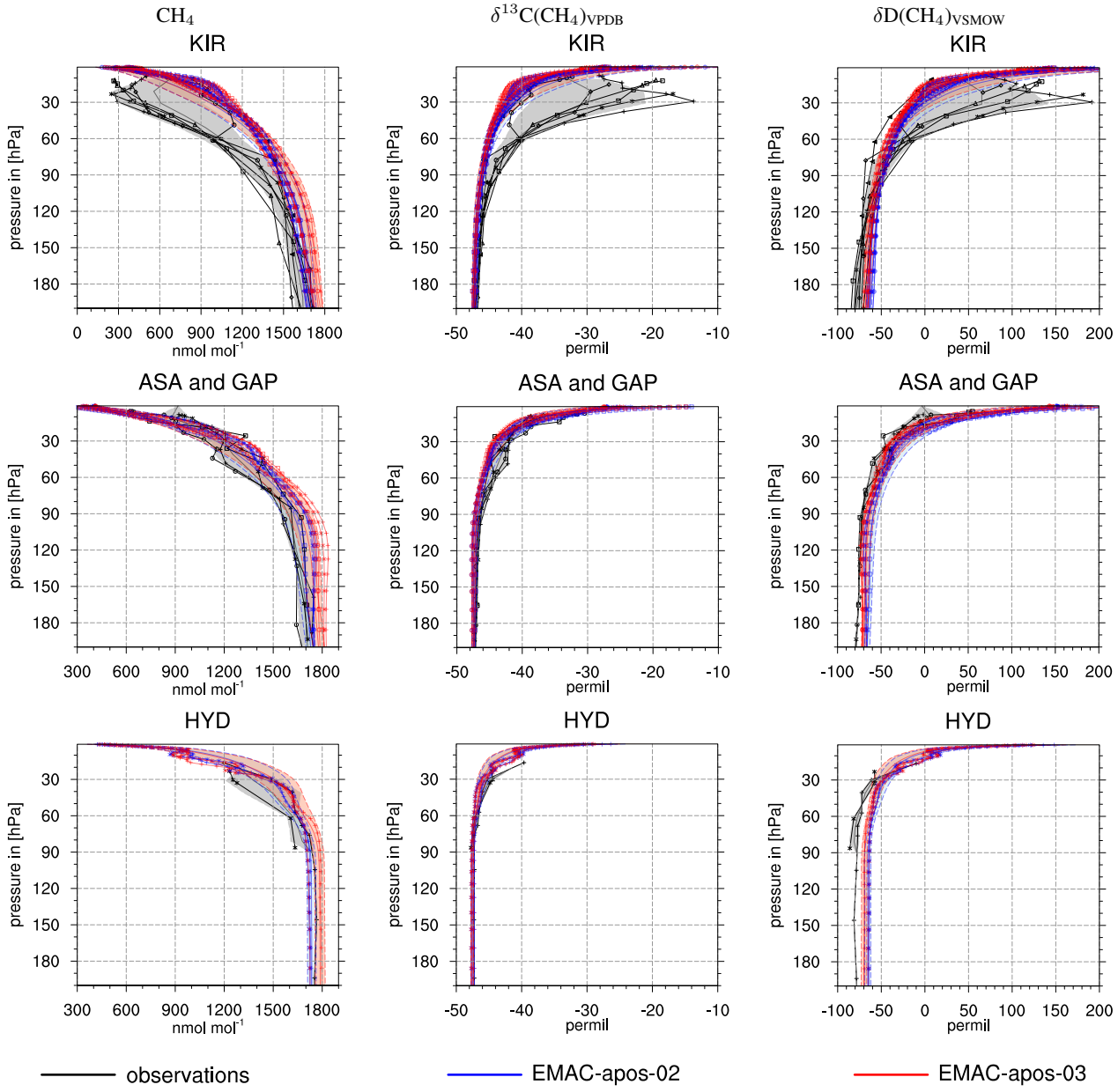

Figure S5. Balloon borne observations from Röckmann et al. (2011, black) together with simulation results from EMAC-apos-02 (blue) and EMAC-apos-03 (red). The rows of panels from top to bottom present balloon launches in the polar region from Kiruna in Sweden (KIR), in the mid-latitude region from Aire sur l'Adour in France (ASA) and Gap in France (GAP), and in the tropical region from Hyderabad in India (HYD). The profiles of the simulations are taken from monthly averaged data in the specific year, month and at the location of the observation. For observations taken before the simulation start, the simulated year 1990 is shown. Shaded areas indicate the single standard deviation of the observations (grey) and the simulations (blue and red, respectively) with respect to the variations within the specific latitudinal region and the interannual variation in the years 1990–2003.

S3 Documentation of the CH4 submodel

S3.1 Introduction

The CH4 submodel represents a simplified CH_4 chemistry. It defines the tracer `CH4_fx`, which gets reduced via the four CH_4 sink reactions. The tracer is initialized from external data via the submodel TRACER (Jöckel et al., 2008) and modified by either emissions, which need to be introduced via the submodel OFFline EMISsions (OFFEMIS) (Kerkweg et al., 2006) or by Newtonian relaxation towards a lower boundary condition with the submodel TNUDGE (Kerkweg et al., 2006). Example namelist entries concerning the configuration of these submodels are found in Section S5.

Additional to that, the CH4 submodel provides two further options. One is the simulation of the CH_4 isotopologues, and the second is the representation of age and emission classes of CH_4, which, to some extent, are able to resolve an additional spatial and temporal information of the CH_4 emissions.

The option concerning the CH_4 isotopologues can be applied with respect to ^{13}C isotopologues, D isotopologues, or both. The submodel defines the following tracers for the given isotopologues: `CH4_12C` (methane containing carbon-12 (^{12}C, $^{12}CH_4$)), `CH4_13C` ($^{13}CH_4$), `CH4_D0` (CH_4), and `CH4_D1` (CH_3D).

The option to simulate age and emission classes introduces additional tracers depending on the chosen number of age and emission classes. For every combination of age and emission class one tracer is defined, thus, if N is the number of age classes and M is the number of emission classes, in total $N \times M$ additional tracers are defined. The tracers are denoted by the names `CH4_fx_e[mm]_a[nn]`, with `[mm]` being the identifying number of the emission class and `[nn]` the number of the age class.

The following section documents the subroutines, which are part of the CH4 submodel and in the section "User interface" the entries in the corresponding namelists are explained.

S3.2 MODULE messy_ch4_si: Subroutines in the submodel interface layer (SMIL)

These subroutines follow the general structure mandatory for Modular Earth Submodel System (MESSy) submodels. Note that _gp and _lg denote the Gaussian grid point and Lagrangian mode (see Brinkop and Jöckel (2019) for more information). In the presented examples solely the Gaussian grid point mode is used.

- `SUBROUTINE ch4_initialize`: Initializes the submodel, reads the control and coupling namelists and broadcasts the information to all parallel tasks.
- `SUBROUTINE ch4_new_tracer`: Defines the new tracers, which also includes the additional tracers regarding the submodel extensions (if applied).
- `SUBROUTINE ch4_init_memory`: Defines the channel objects and allocates memory.
- `SUBROUTINE ch4_init_coupling`: Sets pointers for coupling to the basemodel and other submodels.
- `SUBROUTINE ch4_global_start`: Sets values of internal variables with respect to the applied ageing method, if the option of age and emission classes is switched on.
- `SUBROUTINE ch4_vdiff`: Currently not used.
- `SUBROUTINE ch4_physc`: This subroutine calls the integration step of the submodel, i.e. `ch4_integrate`. It further accounts for the water vapour (H_2O) feedback, if it is switched on. The tendencies for the age and emission class tracers and the isotopologue tracers are calculated in separate integration routines, namely `class_integrate_gp/lg` and `iso_integrate_gp/lg`.
- `SUBROUTINE ch4_global_end`: Entry point in time loop for LG calculations; not used for the presented examples.
- `SUBROUTINE ch4_free_memory`: Deallocation of allocated memory.

S3.3 MODULE messy_ch4: Subroutines in the submodel core layer (SMCL)

The following subroutines represent the core layer of the submodel.

SUBROUTINE ch4_integrate		(CH4_te, CH4, OH, O1D, Cl, j_CH4, temp, press, spechum, iso_id)	
name	type	intent	description
mandatory arguments:			
CH4_te	REAL	OUT	CH_4 tendency
CH4	REAL	IN	CH_4 mixing ratio
OH	REAL	IN	OH mixing ratio
O1D	REAL	IN	$O(^1D)$ mixing ratio
Cl	REAL	IN	Cl mixing ratio
j_CH4	REAL	IN	photolysis rate of CH_4
temp	REAL	IN	temperature
press	REAL	IN	pressure
spechum	REAL	IN	specific humidity
iso_id	INTEGER	IN	ID of isotopologue

description:
This subroutine executes the integration step of the submodel. It applies the functional (i.e. temperature dependent) reaction rate coefficients of the sink reactions of CH_4 and accounts for the KIE in the case of rare isotopologues.

SUBROUTINE sca_tend		(m, mte, s, ste, dt, a)	
name	type	intent	description
mandatory arguments:			
m	REAL	IN	master tracer
mte	REAL	IN	tendency of master tracer
s	REAL	IN	sum of fractional tracers
ste	REAL	IN	sum of fractional tracer tendencies
dt	REAL	IN	time step length
a	REAL	OUT	resulting correction factor

description:
Calculates the necessary correction factor so that the fractional tracers including their tendencies add up to the master tracer (incl. its current tendency).

SUBROUTINE adj_tend			(f, t, a, dt, tadj)
name	type	intent	description
mandatory arguments:			
f	REAL	IN	fractional tracer
t	REAL	IN	tendency of fractional tracer
a	REAL	IN	correction factor
dt	REAL	IN	time step length
tadj	REAL	OUT	resulting additional tendency for adjustment

description:
Calculates the necessary additional tendency to adjust for the given correction factor.

SUBROUTINE ch4_read_nml_ctrl			(status, iou)
name	type	intent	description
mandatory arguments:			
status	INTEGER	OUT	error status info
iou	INTEGER	IN	I/O unit

description:
This subroutine is used to read the CTRL-namelist of the submodel.

S3.4 Private subroutines

Private subroutines in `messy_ch4_si`

SUBROUTINE ch4_read_nml_cpl			(status, iou)
name	type	intent	description
mandatory arguments:			
status	INTEGER	OUT	error status info
iou	INTEGER	IN	I/O unit

description:
This subroutine is used to read the CPL-namelist of the submodel.

SUBROUTINE class_integrate_gp			(temp, press, spechum)
name	type	intent	description
mandatory arguments:			
temp	REAL, DIMENSION(:,:)	IN	temperature
press	REAL, DIMENSION(:,:)	IN	pressure
spechum	REAL, DIMENSION(:,:)	IN	specific humidity

description:
This subroutine calls `ch4_integrate` for every age and emission class tracer separately.

SUBROUTINE class_age_move_gp			(CH4c, CH4c_te)
name	type	intent	description
mandatory arguments:			
CH4c	REAL, DIMENSION(:,:)	IN	current CH_4 tracer mixing ratio
CH4c_te	REAL, DIMENSION(:,:)	IN	current CH_4 tracer tendency
description:			
Accounts for the shifting from one age class to the next.			

SUBROUTINE class_adj_tend_gp			(CH4c, CH4c_te)
name	type	intent	description
mandatory arguments:			
CH4c	REAL, DIMENSION(:,:)	IN	current CH_4 tracer mixing ratio
CH4c_te	REAL, DIMENSION(:,:)	IN	current CH_4 tracer tendency
description:			
Adjusts the tendencies of the age and emission class tracers so that the tracers sum up to the master tracer CH4_fx, which is required to correct for potential numerical inaccuracies.			

SUBROUTINE iso_integrate_gp			(temp, press, spechum, CH4_te)
name	type	intent	description
mandatory arguments:			
temp	REAL, DIMENSION(:,:)	IN	temperature
press	REAL, DIMENSION(:,:)	IN	pressure
spechum	REAL, DIMENSION(:,:)	IN	specific humidity
CH4_te	REAL, DIMENSION(:,:)	IN	current CH_4 tracer tendency
description:			
Calls ch4_integrate for every isotopologue tracer separately. It further calculates the tendency added to the HDO, either by the simple assumption that one HDO molecule is produced by one oxidized CH_3D molecule, or by the function			

$$\frac{\partial(HDO)}{\partial t} = \frac{-\frac{\partial(CH_3D)}{\partial t} + 6.32 \times 10^{-5} \cdot \frac{\partial(CH_4)}{\partial t}}{\frac{M_{air}}{M_{HDO}} \left(\frac{1}{1-HDO}\right)^2}\,, \tag{6}$$

proposed by Eichinger et al. (2015).

SUBROUTINE class_adj_tend_gp			(CH4c, CH4c_te, idt_gp_iso_adj)
name	type	intent	description
mandatory arguments:			
CH4c	REAL, DIMENSION(:)	IN	current CH_4 tracer mixing ratio
CH4c_te	REAL, DIMENSION(:)	IN	current CH_4 tracer tendency
idt_gp_iso_adj	REAL, DIMENSION(:)	IN	list of tracer IDs
description: Adjusts the tendencies of the isotopologue tracers so that the tracers regarding the isotopes of the same element sum up to the master tracer CH4_fx, which is required to correct for potential numerical inaccuracies.			

Private subroutines in `messy_ch4`

SUBROUTINE calc_KIE			(KIE_AB_val, temp_t, KIE_t)
name	type	intent	description
mandatory arguments:			
KIE_AB_val	REAL, DIMENSION(2)	IN	KIE parameters A and B
temp_t	REAL	IN	temperature
KIE_t	REAL	OUT	KIE value
description: Calculates the KIE with the equation: KIE_t = A$\cdot\exp$(B/temp).			

S3.5 User interface

S3.5.1 CH4 CTRL namelist

The control (CTRL) namelist of the CH4 submodel includes the KIE values applied in the isotopologue extension of the submodel for all four sink reactions and both isotopologues.

The KIE is represented in the form KIE = A$\cdot\exp$(B/T), with A and B being the individual parameters and T the temperature in [K]. The namelist entries are given therefore as:
KIE_CH4_XX_YY = A, B.
XX and YY are set according to the specified reaction. XX denotes thereby the isotope in CH_4 and is 13C or D1. YY defines the reaction partner (either OH, O1D or CL) as well as the photolysis with jval. For those KIE, which are temperature independent, B is set to 0.0. The default values are A = 1.0 and B = 0.0, so that no KIE is applied.

S3.5.2 CH4 CPL namelist

The coupling (CPL) namelist of the CH4 submodel sets the parameters for the applied extensions and feedback on the specific humidity. It further determines the channel objects used as the reaction partners in the CH_4 oxidation.

- i_H2O_feedback takes an integer, which controls the feedback of CH_4 oxidation on the specific humidity. Allowed values are: 0: no feedback, 1: feedback from GP and 2: feedback from LG. GP and LG denote grid-point representation and Lagrangian representation, respectively. (Default: 0)
- l_ef_re is a logical switch indicating whether the empirical formula introduced by Eichinger et al. (2015) is used (T) or not (F). (Default: F)

- L_GP and L_LG are both logical switches implying whether the Gaussian representation (GP) or Lagrangian representation (LG), or both are applied. The following namelist entries are shown for GP, however, there a identical entries for LG as well (indicated by gp and lg, respectively). (Default: L_GP = T, L_LG = F)

- c_gp_OH, c_gp_O1D, c_gp_Cl and c_gp_jCH4 define the chosen channel objects for the reaction partners of CH_4. They take two strings, the first indicates the channel, the second the object name.

- i_gp_nclass_emis_age denotes the number of emission- and age classes. It takes two integers, the first is the number of emission classes, the second is the number of age classes. (Default: i_gp_nclass_emis_age = 0, 0,)

- r_gp_age_cll is an optional entry, which adjusts the time period (in days) of one age class. This entry is only valid for ageing option 1 and 2 (see main text section 3.1). (Default: 30.44 for each age class)

- l_gp_adj_tend is a logical switch, which indicates whether the tendencies are adjusted so that the additional age and emission class tracers sum up to the master tracer CH4_fx. (Default: T)

- i_gp_ageing is an integer switch indicating the ageing method, which means the advancing of CH_4 from one age class to the next older one. It can be chosen between:

  - 0: monthly in one step
  - 1: continuously (default)
  - 2: monthly

  Note, using the first one, the Leapfrog time stepping with the Asselin-filter might cause numerical oscillations with negative values. Furthermore, the last one is not conform with the submodel TENDENCY, hence the corresponding diagnostic output created by TENDENCY is not meaningful. (Default: 1)

- l_gp_iso_C and l_gp_iso_H are logical switches. indicating whether the isotopologues of CH_4 concerning ^{13}C, D, or both are simulated. (Default: .FALSE.)

S3.6 Example namelist

Namelist 1. Control (CTRL) and coupling (CPL) namelist of submodel CH4, stored in ch4.nml

```
&CTRL
!! ### KIE values for isotopologues
!! ### SYNTAX:
!! ###   KIE_*    = A, B,
!! ### with KIE(T) = A * exp(B/T)
!! ### temperature independent for B = 0._dp
!! ###
!! ### Reference KIE values:
!! ### Carbon 13 and D kinetic isotope effects in the reactions of CH4
!! ### with O1(D) and OH: New laboratory measurements and their
!! ### implications for the isotopic composition of stratospheric
!! ### methane
!! ### G. Saueressig, J. Crowley, P. Bergamaschi, C. Bruehl,
!! ### C.A.M. Brenninkmeijer and H. Fischer
!! ### [2001] Journal of Geosphysical Research
KIE_CH4_13C_OH  = 1.0039, 0.0,
KIE_CH4_13C_O1D = 1.013 , 0.0,
KIE_CH4_13C_CL  = 1.043 , 6.455,
KIE_CH4_13C_jval = 1.0 , 0.0,
KIE_CH4_D1_OH   = 1.097 , 49.0,
KIE_CH4_D1_O1D  = 1.060 , 0.0,
```

```
KIE_CH4_D1_CL   = 1.278 , 51.31,
KIE_CH4_D1_jval = 1.0, 0.0,
!
/
!
&CPL
!! ### feed back H2O tendency (= -2 * CH4-tendency) into specfic humidity?
!! ### (0: no feedback; 1: feedback from GP; 2: feedback from LG)
i_H2O_feedback = 1,
!! ### grid-point calculation
L_GP = T,
! L_LG = T,
!! ### educts and photolysis rate
c_gp_OH   = 'import_grid', 'CH4OX_OH',
c_gp_O1D  = 'import_grid', 'CH4OX_O1D',
c_gp_Cl   = 'import_grid', 'CH4OX_Cl',
c_gp_jCH4 = 'jval_gp',     'J_CH4',
!
! flag for empirical formula of Eichinger et al. (2015)
l_ef_re = T,
!
! ########################################################
! ### ADDITIONAL SECTION FOR EMISSION AND AGE CLASSES ###
! ########################################################
!
! ### n emission x m age classes
i_gp_nclass_emis_age = 48, 4, ! CAREFUL: If age / emis classes are changed
                              ! here, the tracer.nml must be updated
                              ! apropriately!
                              ! For emissions check offemis.nml,too
! ### age class duration [days] (only for ageing method 1)
!r_gp_age_cll = 1.0, 1.0, 1.0, 1.0,          ! for testing
!r_gp_age_cll = 30.44, 30.44, 30.44,30.44,  ! default
! ### adjust tendencies to sum tracer (default: true)
!l_gp_adj_tend = T,
! ### ageing method (0: monthly in one step, 1: continuous (default),
! ###                2: monthly, not TENDENCY conform)
!i_gp_ageing = 1,
i_gp_ageing = 2,
!
! ### n emission x m age classes
! i_lg_nclass_emis_age = 6, 4,
! ### age class duration [days] (only for ageing method 1)
!r_lg_age_cll = 1.0, 1.0, 1.0, 1.0,          ! for testing
!r_lg_age_cll = 30.44, 30.44, 30.44,30.44,   !
! ### adjust tendencies to sum tracer (default: true)
!l_lg_adj_tend = T,
! ### ageing method (0: monthly in one step, 1: continuous (default),
! ###                2: monthly, not TENDENCY conform)
!i_lg_ageing = 1,
! i_lg_ageing = 2,
!
! ###########################################
! ### ADDITIONAL SECTION FOR ISOTOPOLOGUES ###
! ###########################################
!
! ### Switch for isotopologues (GP)
l_gp_iso_C = .TRUE.
l_gp_iso_H = .TRUE.
! ### Switch for isotopologues (LG)
! l_lg_iso_C = .TRUE.
```

```
! l_lg_iso_H = .TRUE.
/
```

S4 Documentation of the TRSYNC submodel

S4.1 Introduction

The submodel TRacer SYNChronization (TRSYNC) guarantees that the physical H_2O tracers (incl. their isotopologues) receive also the correct tendencies of the corresponding chemical tracers.

The submodel CH4 defines the tracer `HDO`, the submodel H_2O ISOtopologues (H2OISO) defines `H2OISOHDOvap`, and the MECCA_TAG in the MECCA defines `I2H2O` (or a different idiom, chosen by the user). The auxiliary submodel TRSYNC couples these tracers to combine the physical and chemical isotopic fractionation.

Without any isotopological extension solely the fifth-generation European Centre Hamburg general circulation model (ECHAM5) intrinsic tracer for specific humidity (q) is present. In this case, chemically produced H_2O (either from CH4 or from MECCA) directly adds optionally to q. However, in case of an isotopological extension using H2OISO, CH4 and/or MECCA_TAG the following additional tracers are defined:

- `H2OISOHHOvap` and `H2OISOHDOvap` (defined by H2OISO): The former is the total water tracer and the latter is the tracer of the rare isotopologue. Note that in H2OISO the two tracers do not add up to a master tracer, actually, `H2OISOHHOvap` represents and is identical to the master tracer (i.e. q).
- `HDO` (defined by CH4).
- `I1H2O` and `I2H2O`, representing H_2O and HDO, respectively (defined by MECCA_TAG): Both sum up to the chemical master tracer `H2O`.
- `H2O` (defined by MECCA): This tracer is originally not defined in MECCA, but is necessary in combination with MECCA_TAG for the internal scaling of `I1H2O` and `I2H2O`.

Figure S6 depicts the schematics of the coupling. At the beginning of every time step, `H2OISOHHOvap` is set to the current value of q, correcting any numerical deviations of `H2OISOHHOvap` from q caused in the previous time step. Next, basically all tracers are modified by the same physical processes: advection, vertical diffusion and convection. However, for the submodels E5VDIFF, CONVECT and CLOUD the hydrological processes are doubled in H2OISO to allow for isotope effects. The submodel Multi-phase Stratospheric Box Model (MSBM) calculates a tendency for q, which is added to `H2OISOHHOvap` as well. An equivalent tendency is added to `H2OISOHDOvap`, which is derived such that no additional fractionation by the multi-phase stratospheric chemistry is implied.

After all physical processes are complete, the submodel TRSYNC is called. It takes care that all tendencies of the previous (physical) processes of `HDO` and `I2H2O` are deleted and overwritten by the corresponding tendencies of the H2OISO equivalent `H2OISOHDOvap`. `I1H2O` is exceptional, as it must be set to the difference of the total tracer `H2OISOHHOvap` and the rare isotopologue `H2OISOHDOvap`. Note that for technical reasons the tracer `H2OISOHDOvap` is defined as one half of the corresponding chemical isotopological tracers `HDO` and `I2H2O`.

Next CH4 computes the CH_4 oxidation and derives the feedback onto q and HDO. At the very beginning of MECCA, the intrinsic `H2O` tracer is synchronized with q. Before and after the calls of the kinetic solver, `I1H2O` and `I2H2O` are scaled appropriately to add up to `H2O`. After this, the feedback onto H_2O is passed to q. To be precise, the sketch in Fig. S6 suggests that CH4 and MECCA are executed in the same simulation. This is indeed possible, but not necessary and it is important to note that only one of the two can provide the chemical feedback onto q, which can be arranged by corresponding switches in the namelists.

After the chemical processes, TRSYNC synchronizes the tracers `HDO` or `I2H2O` backward onto `H2OISOHDOvap`, and H2OISO also adds the chemical tendency of q to `H2OISOHHOvap`. As a last step H2OISO adjusts the tendency of `H2OISOHHOvap` so that it is conform to the tendency of q.

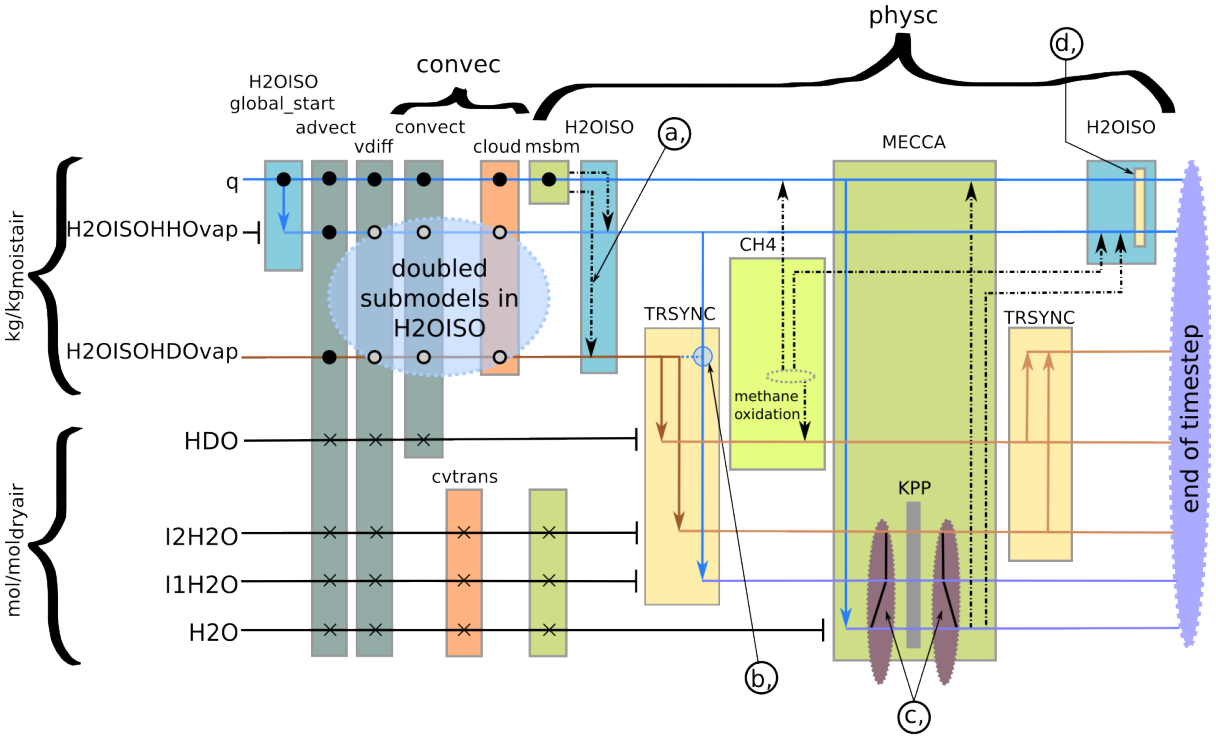

Figure S6. Sketch depicting the coupling of the hydrological cycle tracers in EMAC. q is the intrinsic variable of ECHAM5 for specific humidity. Similar, `H2OISOHHOvap` and `H2OISOHDOvap` are defined by H2OISO. q, `H2OISOHHOvap` and `H2OISOHDOvap` are in units kg of the tracer per kg of moist air (kg $kg^{-1}_{moist\ air}$). `HDO` is defined by CH4, `H2O` is defined by MECCA, and `I1H2O` and `I2H2O` are defined by MECCA-TAG in mol $mol^{-1}_{dry\ air}$. Arrows with dashed lines indicate that solely tendencies are added. Solid arrow lines correspond to a replacement of the contents. (a) relative tendency of MSBM of HHO tracer without fractionation, (b) sets `I1H2O` to the mol $mol^{-1}_{dry\ air}$ equivalent of `H2OISOHHOvap` - 2·`H2OISOHDOvap`, (c) adjusts `I1H2O` and `I2H2O` so that `I1H2O` + `I2H2O` = `H2O`, (d) numerical adjustment to ensure that the tendency of `H2OISOHHOvap` is equal to the tendency of q.

The following section documents the subroutines, which are part of the TRSYNC submodel and in the section "User interface" the entries of the corresponding namelist are explained.

S4.2 MODULE messy_trsync_si: Subroutines in SMIL

These subroutines follow the general structure mandatory for MESSy submodels.

- `SUBROUTINE trsync_initialize`: Initializes the submodel, reads the coupling namelist and broadcasts necessary information to all parallel tasks.
- `SUBROUTINE trsync_init_memory`: Registers the tracers for the TENDENCY submodel, if the latter is applied.
- `SUBROUTINE trsync_init_coupling`: Sets pointers to the used tracers and checks whether the synchronized tracers are identical in terms of their molar mass.
- `SUBROUTINE trsync_init_tracer`: Initializes the tracers, hence checks whether the tracers are already initialized and accounts for a synchronized initial state.

- `SUBROUTINE trsync_physc`: This subroutine is called two times. The first time before the kinetic integrations of CH4 and MECCA and the second time after. It provides the necessary unit conversion and numerical adjustment to synchronize the chosen tracers.
- `SUBROUTINE trsync_free_memory`: Currently not necessary.

S4.3 MODULE messy_trsync: Subroutines in SMCL

The following subroutines represent the core layer of the submodel.

SUBROUTINE convert_unit		(traten, case, type, molarmass, spechum, spechum_te, tracer)	
name	type	intent	description
mandatory arguments:			
traten	REAL	INOUT	tracer or tendency to be converted
case	INTEGER	IN	case of conversion (1: kg/kg⇒mol/mol or 2: mol/mol⇒kg/kg)
type	INTEGER	IN	type of conversion (1: tracer or 2: tendency)
molarmass	REAL	IN	molar mass of the converted tracer
spechum	REAL	IN	specific humidity
optional arguments:			
spechum_te	REAL	IN	tendency of specific humidity
tracer	REAL	IN	additional tracer mixing ratio if traten indicates the tendency
description: This subroutine calls the private subroutines convert_to_molmol, convert_to_kgkg, convert_to_molmol_te and convert_to_kgkg_te, depending on the chosen case and type.			

S4.4 Private subroutines

Private subroutines in `messy_trsync_si`

SUBROUTINE trsync_read_nml_cpl		(status, iou)	
name	type	intent	description
mandatory arguments:			
status	INTEGER	OUT	error status info
iou	INTEGER	IN	I/O unit
description: This subroutine is used to read the CPL-namelist of the submodel.			

Private subroutines in `messy_trsync`

SUBROUTINE convert_to_kgkg			(tr_a, molarmass, spechum)
name	type	intent	description
mandatory arguments:			
tr_a	REAL	INOUT	tracer in mol $\text{mol}^{-1}_{\text{dry air}}$ to be converted
molarmass	REAL	IN	molar mass of the converted tracer
spechum	REAL	IN	specific humidity
description:			
This subroutine converts the tracer tr_a from mol $\text{mol}^{-1}_{\text{dry air}}$ to kg $\text{kg}^{-1}_{\text{moist air}}$.			

SUBROUTINE convert_to_molmol			(tr_b, molarmass, spechum)
name	type	intent	description
mandatory arguments:			
tr_b	REAL	INOUT	tracer in kg $\text{kg}^{-1}_{\text{moist air}}$ to be converted
molarmass	REAL	IN	molar mass of the converted tracer
spechum	REAL	IN	specific humidity
description:			
This subroutine converts the tracer tr_b from kg $\text{kg}^{-1}_{\text{moist air}}$ to mol $\text{mol}^{-1}_{\text{dry air}}$.			

SUBROUTINE convert_kgkg_te			(tr_a_te, tr_a, molarmass, spechum, spechum_te)
name	type	intent	description
mandatory arguments:			
tr_a_te	REAL	INOUT	tendency in mol $\text{mol}^{-1}_{\text{dry air}}$ s^{-1} to be converted
tr_a	REAL	IN	corresponding tracer of tendency to be converted
molarmass	REAL	IN	molar mass of the converted tracer
spechum	REAL	IN	specific humidity
spechum_te	REAL	IN	tendency of specific humidity
description:			
This subroutine converts the tendency tr_a_te from mol $\text{mol}^{-1}_{\text{dry air}}$ s^{-1} to kg $\text{kg}^{-1}_{\text{moist air}}$ s^{-1}.			

SUBROUTINE convert_molmol_te			(tr_b_te, tr_b, molarmass, spechum, spechum_te)
name	type	intent	description
mandatory arguments:			
tr_b_te	REAL	INOUT	tendency in kg $kg^{-1}_{moist\ air}$ s^{-1} to be converted
tr_b	REAL	IN	corresponding tracer of tendency to be converted
molarmass	REAL	IN	molar mass of the converted tracer
spechum	REAL	IN	specific humidity
spechum_te	REAL	IN	tendency of specific humidity
description:			
This subroutine converts the tendency tr_b_te from kg $kg^{-1}_{moist\ air}$ s^{-1} to mol $mol^{-1}_{dry\ air}$ s^{-1}.			

S4.5 User interface

S4.5.1 TRSYNC CPL namelist

The coupling (CPL) namelist of the TRSYNC submodel lists the tracers to be synchronized.

TRSYNC takes two strings and one integer switch. The first string indicates the chemical tracer in mol $mol^{-1}_{dry\ air}$. The second string indicates the physical tracer in kg $kg^{-1}_{moist\ air}$. The integer string denotes, whether the synchronization is done in both ways (0), the chemical tracer is synchronized by the physical tracer before chemistry only (1), or the physical tracer is synchronized by the chemical tracer after chemistry (2).

S4.6 Example namelist

Namelist 2. Control (CTRL) and coupling (CPL) namelists of submodel TRSYNC stored in trsync.nml

```
&CTRL
/
!
&CPL
!! ### List of tracer which should be synchronized by TRSYNC
!! ###
!! ### TRSYNC : synchronization of HDO tracer
!! ### TRSYNC(1) = 'TR_A','TR_B',i
!! ### with:
!! ###       TR_A in mol/mol_dryair
!! ###       TR_B in kg/kg_moistair
!! ###
!! ### i = 0: both ways (default)
!! ###     1: chemical tracer is synchronized with physical tracer only
!! ###     2: physical tracer is synchronized with chemical tracer only
!! ###
!! ### trsync_physc(1) will synchronize TR_A with TR_B (=> TR_A will be overwritten)
!! ### trsync_physc(2) will synchronize TR_B with TR_A (=> TR_B will be overwritten)
!! ###
TRSYNC(1) = 'HDO', 'H2OISOHDOvap',
!! ### TRSYNC(1) = 'I2H2O', 'H2OISOHDOvap', 0,
!! ### Future:
!! ### TRSYNC(2) = '','H2OISOHH18Ovap', 0,
!! ### TRSYNC(3) = '','H2OISOHH17Ovap', 0,
/
```

S5 Example namelist entries for other submodels corresponding to CH4 set-up

The following snippets show namelist entries of other submodels for a MESSy set-up with the CH4 submodel.

S5.1 TRACER

Namelist 3. Part of tracer.nml to import initial values of CH_4 tracer.

```
! Import from first spin-up
&regrid
infile    = "~/EMAC-x-02_____0013_restart_0005_tracer_gp.nc",  ! 2010-12-31 23:48 ...
i_latm    = "lat",          ! name of latitude axis in input file
i_latr    = -90.0,90.0,     ! range of latitude axis in input file
i_lonm    = "lon",          ! name of longitude axis in input file
i_lonr    = 0.0,360.0,      ! range of longitude axis in input file
! No time coordinate in restart files
!i_timem   = "time",         ! name of time axis in input file
i_hyam    = "hyam",     ! name of hybrid A coefficients in input file
i_hybm    = "hybm",     ! name of hybrid B coefficients in input file
i_ps      = "101325.0 Pa",
i_p0      = "1. Pa",        ! value of reference pressure in input file
pressure  = F,
! Use ALL tracers in init file
!var       =  "CH4_fx;CH4_12C;CH4_13C;CH4_D0;CH4_D1", ! CH4 tracers
! No time coordinate in restart files
!i_t       = 25,
/
```

S5.2 DDEP

Namelist 4. Configuration of ddep.nml to simulate soil-loss of CH_4.

```
!## SYNTAX:
!## import_predepvel(.) = 'channel', 'object', 'tracer-name', diag. flux calc.?
!## Note: channel object is deposition flux aand must be in [molec/m^2/s]
!
!
import_predepvel(1) = 'import_grid', 'DVMETH_oxid', 'CH4_fx', T,
import_predepvel(2) = 'import_grid', 'DVMETH_oxid', 'CH4_D0', T,
import_predepvel(3) = 'import_grid', 'DVMETH_CH3D_oxid', 'CH4_D1', T,
import_predepvel(4) = 'import_grid', 'DVMETH_13CH4_oxid', 'CH4_13C', T,
import_predepvel(5) = 'import_grid', 'DVMETH_oxid', 'CH4_12C', T,
!
```

S5.3 IMPORT

Namelist 5. Entries of import.nml, which import the educts (OH, Cl and $O(^1D)$) from an earlier simulation and the CH_4 emission inventory for each emission class.

```
! ##########################################################################
! CH4
! ##########################################################################
!
! PRESCRIBED EDUCTS (CH + ...): OH, O1D, Cl for methane oxidation
! QCTM data starts at Dec 1978 and ends at Nov 2014
RG_TRIG(3)  = 1,'months', 'first',0, 'CH4OX',  422,1,432,134,
```

```
       'NML=./import/MISC/QCTM/ESCiMo_DLR1.0_RC1SD-base-10_4QCTM_misc_197901-201412.nml;',
!
! ########################################################################
! OFFEMIS
! ########################################################################
!
! CH4_fx emissions
!
! biomass burning
RG_TRIG(20)  = 1,  'months', 'first',0, 'BB_AUS',        265,1,276,1,
       'NML=./import/offemis/CH4/EMPA/EMPA_DLR1.1_PostE_bb+AUS_CH4_199001-201212.nml; VAR=CH4;',
RG_TRIG(21)  = 1,  'months', 'first',0, 'BB_CHINA',      265,1,276,1,
       'NML=./import/offemis/CH4/EMPA/EMPA_DLR1.1_PostE_bb+CHINA_CH4_199001-201212.nml; VAR=CH4;',
RG_TRIG(22)  = 1,  'months', 'first',0, 'BB_EU',         265,1,276,1,
       'NML=./import/offemis/CH4/EMPA/EMPA_DLR1.1_PostE_bb+EU_CH4_199001-201212.nml; VAR=CH4;',
RG_TRIG(23)  = 1,  'months', 'first',0, 'BB_INDIA',      265,1,276,1,
       'NML=./import/offemis/CH4/EMPA/EMPA_DLR1.1_PostE_bb+INDIA_CH4_199001-201212.nml; VAR=CH4;',
RG_TRIG(24)  = 1,  'months', 'first',0, 'BB_NA_bor',     265,1,276,1,
       'NML=./import/offemis/CH4/EMPA/EMPA_DLR1.1_PostE_bb+NAbor_CH4_199001-201212.nml; VAR=CH4;',
RG_TRIG(25)  = 1,  'months', 'first',0, 'BB_N_AFR',      265,1,276,1,
       'NML=./import/offemis/CH4/EMPA/EMPA_DLR1.1_PostE_bb+NAFR_CH4_199001-201212.nml; VAR=CH4;',
RG_TRIG(26)  = 1,  'months', 'first',0, 'BB_NA_temp',    265,1,276,1,
       'NML=./import/offemis/CH4/EMPA/EMPA_DLR1.1_PostE_bb+NAtemp_CH4_199001-201212.nml; VAR=CH4;',
RG_TRIG(27)  = 1,  'months', 'first',0, 'BB_N_MIDEAST',  265,1,276,1,
       'NML=./import/offemis/CH4/EMPA/EMPA_DLR1.1_PostE_bb+NMIDEAST_CH4_199001-201212.nml; VAR=CH4;',
RG_TRIG(28)  = 1,  'months', 'first',0, 'BB_RUS',        265,1,276,1,
       'NML=./import/offemis/CH4/EMPA/EMPA_DLR1.1_PostE_bb+RUS_CH4_199001-201212.nml; VAR=CH4;',
RG_TRIG(29)  = 1,  'months', 'first',0, 'BB_S_AFR',      265,1,276,1,
       'NML=./import/offemis/CH4/EMPA/EMPA_DLR1.1_PostE_bb+SAFR_CH4_199001-201212.nml; VAR=CH4;',
RG_TRIG(30)  = 1,  'months', 'first',0, 'BB_SA_temp',    265,1,276,1,
       'NML=./import/offemis/CH4/EMPA/EMPA_DLR1.1_PostE_bb+SAtemp_CH4_199001-201212.nml; VAR=CH4;',
RG_TRIG(31)  = 1,  'months', 'first',0, 'BB_SA_trop',    265,1,276,1,
       'NML=./import/offemis/CH4/EMPA/EMPA_DLR1.1_PostE_bb+SAtrop_CH4_199001-201212.nml; VAR=CH4;',
RG_TRIG(32)  = 1,  'months', 'first',0, 'BB_SE_ASIA',    265,1,276,1,
       'NML=./import/offemis/CH4/EMPA/EMPA_DLR1.1_PostE_bb+SEASIA_CH4_199001-201212.nml; VAR=CH4;',
!
! anthropogenic
!
RG_TRIG(140) = 1,  'months',  'first',0, 'Mfx_an_AFRICA',  265,1,276,1,
       'NML=./import/offemis/CH4/EMPA/EMPA_DLR1.1_PostE_anth+AFRICA_CH4_199001-201212.nml; VAR=CH4;',
RG_TRIG(141) = 1,  'months',  'first',0, 'Mfx_an_AUS',     265,1,276,1,
       'NML=./import/offemis/CH4/EMPA/EMPA_DLR1.1_PostE_anth+AUS_CH4_199001-201212.nml; VAR=CH4;',
RG_TRIG(142) = 1,  'months',  'first',0, 'Mfx_an_CHINA',   265,1,276,1,
       'NML=./import/offemis/CH4/EMPA/EMPA_DLR1.1_PostE_anth+CHINA_CH4_199001-201212.nml; VAR=CH4;',
RG_TRIG(143) = 1,  'months',  'first',0, 'Mfx_an_EU',      265,1,276,1,
       'NML=./import/offemis/CH4/EMPA/EMPA_DLR1.1_PostE_anth+EU_CH4_199001-201212.nml; VAR=CH4;',
RG_TRIG(144) = 1,  'months',  'first',0, 'Mfx_an_INDIA',   265,1,276,1,
       'NML=./import/offemis/CH4/EMPA/EMPA_DLR1.1_PostE_anth+INDIA_CH4_199001-201212.nml; VAR=CH4;',
RG_TRIG(145) = 1,  'months',  'first',0, 'Mfx_an_MIDEAST', 265,1,276,1,
       'NML=./import/offemis/CH4/EMPA/EMPA_DLR1.1_PostE_anth+MIDEAST_CH4_199001-201212.nml; VAR=CH4;',
RG_TRIG(146) = 1,  'months',  'first',0, 'Mfx_an_NA',      265,1,276,1,
       'NML=./import/offemis/CH4/EMPA/EMPA_DLR1.1_PostE_anth+NA_CH4_199001-201212.nml; VAR=CH4;',
RG_TRIG(147) = 1,  'months',  'first',0, 'Mfx_an_OCEAN',   265,1,276,1,
       'NML=./import/offemis/CH4/EMPA/EMPA_DLR1.1_PostE_ship_CH4_199001-201212.nml; VAR=CH4;',
RG_TRIG(148) = 1,  'months',  'first',0, 'Mfx_an_RUS',     265,1,276,1,
       'NML=./import/offemis/CH4/EMPA/EMPA_DLR1.1_PostE_anth+RUS_CH4_199001-201212.nml; VAR=CH4;',
RG_TRIG(149) = 1,  'months',  'first',0, 'Mfx_an_SA',      265,1,276,1,
       'NML=./import/offemis/CH4/EMPA/EMPA_DLR1.1_PostE_anth+SA_CH4_199001-201212.nml; VAR=CH4;',
RG_TRIG(150) = 1,  'months',  'first',0, 'Mfx_an_SE_ASIA', 265,1,276,1,
       'NML=./import/offemis/CH4/EMPA/EMPA_DLR1.1_PostE_anth+SEASIA_CH4_199001-201212.nml; VAR=CH4;',
!
```

```
! ocean
!
RG_TRIG(151) = 1,  'months',  'first',0, 'Mfx_oc',         265,1,276,1,
       'NML=./import/offemis/CH4/EMPA/EMPA_DLR1.1_PostE_ocean_CH4_199001-201212.nml; VAR=CH4;',
!
! rice
!
RG_TRIG(152) = 1,  'months', 'first',0, 'Mfx_ri_AFR',      265,1,276,1,
       'NML=./import/offemis/CH4/EMPA/EMPA_DLR1.1_PostE_rice+AFR_CH4_199001-201212.nml; VAR=CH4;',
RG_TRIG(153) = 1,  'months', 'first',0, 'Mfx_ri_ASIA_AUS', 265,1,276,1,
       'NML=./import/offemis/CH4/EMPA/EMPA_DLR1.1_PostE_rice+ASIA+AUS_CH4_199001-201212.nml; VAR=CH4;',
RG_TRIG(154) = 1,  'months', 'first',0, 'Mfx_ri_CHINA',    265,1,276,1,
       'NML=./import/offemis/CH4/EMPA/EMPA_DLR1.1_PostE_rice+CHINA_CH4_199001-201212.nml; VAR=CH4;',
RG_TRIG(155) = 1,  'months', 'first',0, 'Mfx_ri_EU',       265,1,276,1,
       'NML=./import/offemis/CH4/EMPA/EMPA_DLR1.1_PostE_rice+EU_CH4_199001-201212.nml; VAR=CH4;',
RG_TRIG(156) = 1,  'months', 'first',0, 'Mfx_ri_INDIA',    265,1,276,1,
       'NML=./import/offemis/CH4/EMPA/EMPA_DLR1.1_PostE_rice+INDIA_CH4_199001-201212.nml; VAR=CH4;',
RG_TRIG(157) = 1,  'months', 'first',0, 'Mfx_ri_NA',       265,1,276,1,
       'NML=./import/offemis/CH4/EMPA/EMPA_DLR1.1_PostE_rice+NA_CH4_199001-201212.nml; VAR=CH4;',
RG_TRIG(158) = 1,  'months', 'first',0, 'Mfx_ri_SA',       265,1,276,1,
       'NML=./import/offemis/CH4/EMPA/EMPA_DLR1.1_PostE_rice+SA_CH4_199001-201212.nml; VAR=CH4;',
!
! termites
!
RG_TRIG(159) = 1,  'months',  'first',0, 'Mfx_te',         265,1,276,1,
       'NML=./import/offemis/CH4/EMPA/EMPA_DLR1.1_PostE_biotermites_CH4_199001-201212.nml; VAR=CH4;',
!
! volcanoes
!
RG_TRIG(160) = 1,  'months',  'first',0, 'Mfx_vo',         265,1,276,1,
       'NML=./import/offemis/CH4/EMPA/EMPA_DLR1.1_PostE_volc_CH4_199001-201212.nml; VAR=CH4;',
!
! wetlands
!
RG_TRIG(161) = 1,  'months', 'first',0, 'Mfx_wl_AUS',     265,1,276,1,
       'NML=./import/offemis/CH4/EMPA/EMPA_DLR1.1_PostE_biowetlands+AUS_CH4_199001-201212.nml; VAR=CH4;',
RG_TRIG(162) = 1,  'months', 'first',0, 'Mfx_wl_CHINA',   265,1,276,1,
       'NML=./import/offemis/CH4/EMPA/EMPA_DLR1.1_PostE_biowetlands+CHINA_CH4_199001-201212.nml; VAR=CH4;',
RG_TRIG(163) = 1,  'months', 'first',0, 'Mfx_wl_EU',      265,1,276,1,
       'NML=./import/offemis/CH4/EMPA/EMPA_DLR1.1_PostE_biowetlands+EU_CH4_199001-201212.nml; VAR=CH4;',
RG_TRIG(164) = 1,  'months', 'first',0, 'Mfx_wl_india',   265,1,276,1,
       'NML=./import/offemis/CH4/EMPA/EMPA_DLR1.1_PostE_biowetlands+INDIA_CH4_199001-201212.nml; VAR=CH4;',
RG_TRIG(165) = 1,  'months', 'first',0, 'Mfx_wl_MIDEAST', 265,1,276,1,
       'NML=./import/offemis/CH4/EMPA/EMPA_DLR1.1_PostE_biowetlands+MIDEAST_CH4_199001-201212.nml; VAR=CH4;',
RG_TRIG(166) = 1,  'months', 'first',0, 'Mfx_wl_NA_bor',  265,1,276,1,
       'NML=./import/offemis/CH4/EMPA/EMPA_DLR1.1_PostE_biowetlands+NAbor_CH4_199001-201212.nml; VAR=CH4;',
RG_TRIG(167) = 1,  'months', 'first',0, 'Mfx_wl_N_AFR',   265,1,276,1,
       'NML=./import/offemis/CH4/EMPA/EMPA_DLR1.1_PostE_biowetlands+NAFR_CH4_199001-201212.nml; VAR=CH4;',
RG_TRIG(168) = 1,  'months', 'first',0, 'Mfx_wl_NA_TEMP', 265,1,276,1,
       'NML=./import/offemis/CH4/EMPA/EMPA_DLR1.1_PostE_biowetlands+NAtemp_CH4_199001-201212.nml; VAR=CH4;',
RG_TRIG(169) = 1,  'months', 'first',0, 'Mfx_wl_RUS',     265,1,276,1,
       'NML=./import/offemis/CH4/EMPA/EMPA_DLR1.1_PostE_biowetlands+RUS_CH4_199001-201212.nml; VAR=CH4;',
RG_TRIG(170) = 1,  'months', 'first',0, 'Mfx_wl_S_AFR',   265,1,276,1,
       'NML=./import/offemis/CH4/EMPA/EMPA_DLR1.1_PostE_biowetlands+SAFR_CH4_199001-201212.nml; VAR=CH4;',
RG_TRIG(171) = 1,  'months', 'first',0, 'Mfx_wl_SA_temp', 265,1,276,1,
       'NML=./import/offemis/CH4/EMPA/EMPA_DLR1.1_PostE_biowetlands+SAtemp_CH4_199001-201212.nml; VAR=CH4;',
RG_TRIG(172) = 1,  'months', 'first',0, 'Mfx_wl_SA_TROP', 265,1,276,1,
       'NML=./import/offemis/CH4/EMPA/EMPA_DLR1.1_PostE_biowetlands+SAtrop_CH4_199001-201212.nml; VAR=CH4;',
RG_TRIG(173) = 1,  'months', 'first',0, 'Mfx_wl_se_asia', 265,1,276,1,
       'NML=./import/offemis/CH4/EMPA/EMPA_DLR1.1_PostE_biowetlands+SEASIA_CH4_199001-201212.nml; VAR=CH4;',
!
```

```
! wild animals
!
RG_TRIG(174) = 1,   'months',  'first',0, 'Mfx_wa',         265,1,276,1,
        'NML=./import/offemis/CH4/EMPA/EMPA_DLR1.1_PostE_wildlife_CH4_199001-201212.nml; VAR=CH4;',
!
```

S5.4 OFFEMIS

Namelist 6. Example of the offemis.nml, which couples the imported emissions to the master CH_4 tracer `CH4_fx`, to the isotopologues, scaled according to the emission signature, and to the corresponding emission class tracers.

```
! ### SYNTAX:
!     (SPECIFIERS MUST BE UPPERCASE !)
! ###         GP=    Gridpoint  Emission Method (0,1,2) (SURFACE ONLY)
!                    0: no emission; only channel object (DEFAULT)
!                    1: 2D (SURFACE EM.) -> lowest layer
!                       3D (VOLUME  EM.) -> emission ON
!                       Nx2D (MULTI LEVEL EM.) -> internally converted to 3D
!                    SURFACE EMISSIONS ONLY:
!                    2: lower boundary condition for flux
!
! ###         LG=    Lagrangian Emission Method (0,1,2,3,4)
!                    0: no emission; only channel object (DEFAULT)
!                    1: 2D (SURFACE EM.)       -> into CELLs in lowest layer
!                       3D (VOLUME  EM.)       -> emission ON
!                       Nx2D (MULTI LEVEL EM.) -> internally converted to 3D
!                    SURFACE EMISSIONS ONLY:
!                    2: into lowest CELLs within boundary layer
!                    3: into all CELLs in boundary layer (vertical gradient)
!                    4: into all CELLs in boundary layer (no vertical gradient)
!
!NOTEs:  (1) Surface emission fluxes (2D) must be in  molecules m-2 s-1.
!        (2) Volume emissions (3D)        must be in  molecules m-3 s-1.
!        (3) Multi level emissions (Nx2D) must be in  molecules m-2 s-1.
!        (4) For volume emissions (3D), the corresponding channel object
!            must be in the GP_3D_MID representation
!        (5) The trigger for multi level emissions (Nx2D) is the presence
!            of the channel object attribute heights
!
! EMISSION: 'TRACER[_SUBNAME][,scaling];...', CHANNEL NAME, CHANNEL OBJECT,
!           EMISSION METHOD
!
! LOWER BOUNDARY CONDITIONS (SEE tnudge.nml)
!
! ########################################
! DIRECT EMISSIONS
! ########################################
!
EMIS_IN(190) = 'CH4_fx;CH4_12C,0.9894892;CH4_13C,0.0105108;CH4_D0,0.9995110;CH4_D1,0.0004890;CH4_fx_e01_a01',
                                                          'import_grid', 'Mfx_an_AFRICA_CH4', 'GP=2', ! anth.
EMIS_IN(191) = 'CH4_fx;CH4_12C,0.9894892;CH4_13C,0.0105108;CH4_D0,0.9995110;CH4_D1,0.0004890;CH4_fx_e02_a01',
                                                          'import_grid', 'Mfx_an_AUS_CH4', 'GP=2', ! anth.
EMIS_IN(192) = 'CH4_fx;CH4_12C,0.9894892;CH4_13C,0.0105108;CH4_D0,0.9995110;CH4_D1,0.0004890;CH4_fx_e03_a01',
                                                          'import_grid', 'Mfx_an_CHINA_CH4', 'GP=2', ! anth.
EMIS_IN(193) = 'CH4_fx;CH4_12C,0.9894892;CH4_13C,0.0105108;CH4_D0,0.9995110;CH4_D1,0.0004890;CH4_fx_e04_a01',
                                                          'import_grid', 'Mfx_an_EU_CH4', 'GP=2', ! anth.
EMIS_IN(194) = 'CH4_fx;CH4_12C,0.9894892;CH4_13C,0.0105108;CH4_D0,0.9995110;CH4_D1,0.0004890;CH4_fx_e05_a01',
                                                          'import_grid', 'Mfx_an_INDIA_CH4', 'GP=2', ! anth.
EMIS_IN(195) = 'CH4_fx;CH4_12C,0.9894892;CH4_13C,0.0105108;CH4_D0,0.9995110;CH4_D1,0.0004890;CH4_fx_e06_a01',
                                                          'import_grid', 'Mfx_an_MIDEAST_CH4', 'GP=2', ! anth.
```

```
EMIS_IN(196) = 'CH4_fx;CH4_12C,0.9894892;CH4_13C,0.0105108;CH4_D0,0.9995110;CH4_D1,0.0004890;CH4_fx_e07_a01',
                                                          'import_grid', 'Mfx_an_NA_CH4', 'GP=2', ! anth.
EMIS_IN(197) = 'CH4_fx;CH4_12C,0.9894892;CH4_13C,0.0105108;CH4_D0,0.9995110;CH4_D1,0.0004890;CH4_fx_e08_a01',
                                                          'import_grid', 'Mfx_an_OCEAN_CH4', 'GP=2', ! anth.
EMIS_IN(198) = 'CH4_fx;CH4_12C,0.9894892;CH4_13C,0.0105108;CH4_D0,0.9995110;CH4_D1,0.0004890;CH4_fx_e09_a01',
                                                          'import_grid', 'Mfx_an_RUS_CH4', 'GP=2', ! anth.
EMIS_IN(199) = 'CH4_fx;CH4_12C,0.9894892;CH4_13C,0.0105108;CH4_D0,0.9995110;CH4_D1,0.0004890;CH4_fx_e10_a01',
                                                          'import_grid', 'Mfx_an_SA_CH4', 'GP=2', ! anth.
EMIS_IN(200) = 'CH4_fx;CH4_12C,0.9894892;CH4_13C,0.0105108;CH4_D0,0.9995110;CH4_D1,0.0004890;CH4_fx_e11_a01',
                                                          'import_grid', 'Mfx_an_SE_ASIA_CH4', 'GP=2', ! anth.
!
! biomass burning
!
EMIS_IN(201) = 'CH4_fx;CH4_12C,0.9892048;CH4_13C,0.0107952;CH4_D0,0.9995097;CH4_D1,0.0004903;CH4_fx_e12_a01',
                                                          'import_grid', 'BB_AUS_CH4',     'GP=2', ! bb
EMIS_IN(202) = 'CH4_fx;CH4_12C,0.9892048;CH4_13C,0.0107952;CH4_D0,0.9995097;CH4_D1,0.0004903;CH4_fx_e13_a01',
                                                          'import_grid', 'BB_CHINA_CH4',     'GP=2', ! bb
EMIS_IN(203) = 'CH4_fx;CH4_12C,0.9892048;CH4_13C,0.0107952;CH4_D0,0.9995097;CH4_D1,0.0004903;CH4_fx_e14_a01',
                                                          'import_grid', 'BB_EU_CH4',     'GP=2', ! bb
EMIS_IN(204) = 'CH4_fx;CH4_12C,0.9892048;CH4_13C,0.0107952;CH4_D0,0.9995097;CH4_D1,0.0004903;CH4_fx_e15_a01',
                                                          'import_grid', 'BB_INDIA_CH4',     'GP=2', ! bb
EMIS_IN(205) = 'CH4_fx;CH4_12C,0.9892048;CH4_13C,0.0107952;CH4_D0,0.9995097;CH4_D1,0.0004903;CH4_fx_e16_a01',
                                                          'import_grid', 'BB_NA_bor_CH4',     'GP=2', ! bb
EMIS_IN(206) = 'CH4_fx;CH4_12C,0.9892048;CH4_13C,0.0107952;CH4_D0,0.9995097;CH4_D1,0.0004903;CH4_fx_e17_a01',
                                                          'import_grid', 'BB_N_AFR_CH4',     'GP=2', ! bb
EMIS_IN(207) = 'CH4_fx;CH4_12C,0.9892048;CH4_13C,0.0107952;CH4_D0,0.9995097;CH4_D1,0.0004903;CH4_fx_e18_a01',
                                                          'import_grid', 'BB_NA_temp_CH4',     'GP=2', ! bb
EMIS_IN(208) = 'CH4_fx;CH4_12C,0.9892048;CH4_13C,0.0107952;CH4_D0,0.9995097;CH4_D1,0.0004903;CH4_fx_e19_a01',
                                                          'import_grid', 'BB_N_MIDEAST_CH4',     'GP=2', ! bb
EMIS_IN(209) = 'CH4_fx;CH4_12C,0.9892048;CH4_13C,0.0107952;CH4_D0,0.9995097;CH4_D1,0.0004903;CH4_fx_e20_a01',
                                                          'import_grid', 'BB_RUS_CH4',     'GP=2', ! bb
EMIS_IN(210) = 'CH4_fx;CH4_12C,0.9892048;CH4_13C,0.0107952;CH4_D0,0.9995097;CH4_D1,0.0004903;CH4_fx_e21_a01',
                                                          'import_grid', 'BB_S_AFR_CH4',     'GP=2', ! bb
EMIS_IN(211) = 'CH4_fx;CH4_12C,0.9892048;CH4_13C,0.0107952;CH4_D0,0.9995097;CH4_D1,0.0004903;CH4_fx_e22_a01',
                                                          'import_grid', 'BB_SA_temp_CH4',     'GP=2', ! bb
EMIS_IN(212) = 'CH4_fx;CH4_12C,0.9892048;CH4_13C,0.0107952;CH4_D0,0.9995097;CH4_D1,0.0004903;CH4_fx_e23_a01',
                                                          'import_grid', 'BB_SA_trop_CH4',     'GP=2', ! bb
EMIS_IN(213) = 'CH4_fx;CH4_12C,0.9892048;CH4_13C,0.0107952;CH4_D0,0.9995097;CH4_D1,0.0004903;CH4_fx_e24_a01',
                                                          'import_grid', 'BB_SE_ASIA_CH4',     'GP=2', ! bb
!
! ocean
!
EMIS_IN(214) = 'CH4_fx;CH4_12C,0.9895891;CH4_13C,0.0104109;CH4_D0,0.9995141;CH4_D1,0.0004859;CH4_fx_e25_a01',
                                                          'import_grid', 'Mfx_oc_CH4', 'GP=2', ! ocean
!
! rice
!
EMIS_IN(215) = 'CH4_fx;CH4_12C,0.9896329;CH4_13C,0.0103671;CH4_D0,0.9995791;CH4_D1,0.0004209;CH4_fx_e26_a01',
                                                          'import_grid', 'Mfx_ri_AFR_CH4', 'GP=2', ! rice
EMIS_IN(216) = 'CH4_fx;CH4_12C,0.9896329;CH4_13C,0.0103671;CH4_D0,0.9995791;CH4_D1,0.0004209;CH4_fx_e27_a01',
                                                          'import_grid', 'Mfx_ri_ASIA_AUS_CH4', 'GP=2', ! rice
EMIS_IN(217) = 'CH4_fx;CH4_12C,0.9896329;CH4_13C,0.0103671;CH4_D0,0.9995791;CH4_D1,0.0004209;CH4_fx_e28_a01',
                                                          'import_grid', 'Mfx_ri_CHINA_CH4', 'GP=2', ! rice
EMIS_IN(218) = 'CH4_fx;CH4_12C,0.9896329;CH4_13C,0.0103671;CH4_D0,0.9995791;CH4_D1,0.0004209;CH4_fx_e29_a01',
                                                          'import_grid', 'Mfx_ri_EU_CH4', 'GP=2', ! rice
EMIS_IN(219) = 'CH4_fx;CH4_12C,0.9896329;CH4_13C,0.0103671;CH4_D0,0.9995791;CH4_D1,0.0004209;CH4_fx_e30_a01',
                                                          'import_grid', 'Mfx_ri_INDIA_CH4', 'GP=2', ! rice
EMIS_IN(220) = 'CH4_fx;CH4_12C,0.9896329;CH4_13C,0.0103671;CH4_D0,0.9995791;CH4_D1,0.0004209;CH4_fx_e31_a01',
                                                          'import_grid', 'Mfx_ri_NA_CH4', 'GP=2', ! rice
EMIS_IN(221) = 'CH4_fx;CH4_12C,0.9896329;CH4_13C,0.0103671;CH4_D0,0.9995791;CH4_D1,0.0004209;CH4_fx_e32_a01',
                                                          'import_grid', 'Mfx_ri_SA_CH4', 'GP=2', ! rice
```

```
!
! termites
!
EMIS_IN(222) = 'CH4_fx;CH4_12C,0.9896366;CH4_13C,0.0103634;CH4_D0,0.9996200;CH4_D1,0.0003800;CH4_fx_e33_a01',
                                                          'import_grid', 'Mfx_te_CH4', 'GP=2', ! termites
!
! volcanoes
!
EMIS_IN(223) = 'CH4_fx;CH4_12C,0.9893910;CH4_13C,0.0106090;CH4_D0,0.9995349;CH4_D1,0.0004651;CH4_fx_e34_a01',
                                                          'import_grid', 'Mfx_vo_CH4', 'GP=2', ! volcanoes
!
! wetlands
!
EMIS_IN(224) = 'CH4_fx;CH4_12C,0.9895934;CH4_13C,0.0104066;CH4_D0,0.9995865;CH4_D1,0.0004135;CH4_fx_e35_a01',
                                                          'import_grid', 'Mfx_wl_AUS_CH4', 'GP=2', ! wetlands
EMIS_IN(225) = 'CH4_fx;CH4_12C,0.9895934;CH4_13C,0.0104066;CH4_D0,0.9995865;CH4_D1,0.0004135;CH4_fx_e36_a01',
                                                          'import_grid', 'Mfx_wl_CHINA_CH4', 'GP=2', ! wetlands
EMIS_IN(226) = 'CH4_fx;CH4_12C,0.9895934;CH4_13C,0.0104066;CH4_D0,0.9995865;CH4_D1,0.0004135;CH4_fx_e37_a01',
                                                          'import_grid', 'Mfx_wl_EU_CH4', 'GP=2', ! wetlands
EMIS_IN(227) = 'CH4_fx;CH4_12C,0.9895934;CH4_13C,0.0104066;CH4_D0,0.9995865;CH4_D1,0.0004135;CH4_fx_e38_a01',
                                                          'import_grid', 'Mfx_wl_india_CH4', 'GP=2', ! wetlands
EMIS_IN(228) = 'CH4_fx;CH4_12C,0.9895934;CH4_13C,0.0104066;CH4_D0,0.9995865;CH4_D1,0.0004135;CH4_fx_e39_a01',
                                                          'import_grid', 'Mfx_wl_MIDEAST_CH4', 'GP=2', ! wetlands
EMIS_IN(229) = 'CH4_fx;CH4_12C,0.9895934;CH4_13C,0.0104066;CH4_D0,0.9995865;CH4_D1,0.0004135;CH4_fx_e40_a01',
                                                          'import_grid', 'Mfx_wl_NA_bor_CH4', 'GP=2', ! wetlands
EMIS_IN(230) = 'CH4_fx;CH4_12C,0.9895934;CH4_13C,0.0104066;CH4_D0,0.9995865;CH4_D1,0.0004135;CH4_fx_e41_a01',
                                                          'import_grid', 'Mfx_wl_N_AFR_CH4', 'GP=2', ! wetlands
EMIS_IN(231) = 'CH4_fx;CH4_12C,0.9895934;CH4_13C,0.0104066;CH4_D0,0.9995865;CH4_D1,0.0004135;CH4_fx_e42_a01',
                                                          'import_grid', 'Mfx_wl_NA_TEMP_CH4', 'GP=2', ! wetlands
EMIS_IN(232) = 'CH4_fx;CH4_12C,0.9895934;CH4_13C,0.0104066;CH4_D0,0.9995865;CH4_D1,0.0004135;CH4_fx_e43_a01',
                                                          'import_grid', 'Mfx_wl_RUS_CH4', 'GP=2', ! wetlands
EMIS_IN(233) = 'CH4_fx;CH4_12C,0.9895934;CH4_13C,0.0104066;CH4_D0,0.9995865;CH4_D1,0.0004135;CH4_fx_e44_a01',
                                                          'import_grid', 'Mfx_wl_S_AFR_CH4', 'GP=2', ! wetlands
EMIS_IN(234) = 'CH4_fx;CH4_12C,0.9895934;CH4_13C,0.0104066;CH4_D0,0.9995865;CH4_D1,0.0004135;CH4_fx_e45_a01',
                                                          'import_grid', 'Mfx_wl_SA_temp_CH4', 'GP=2', ! wetlands
EMIS_IN(235) = 'CH4_fx;CH4_12C,0.9895934;CH4_13C,0.0104066;CH4_D0,0.9995865;CH4_D1,0.0004135;CH4_fx_e46_a01',
                                                          'import_grid', 'Mfx_wl_SA_TROP_CH4', 'GP=2', ! wetlands
EMIS_IN(236) = 'CH4_fx;CH4_12C,0.9895934;CH4_13C,0.0104066;CH4_D0,0.9995865;CH4_D1,0.0004135;CH4_fx_e47_a01',
                                                          'import_grid', 'Mfx_wl_se_asia_CH4', 'GP=2', ! wetlands
!
! wild animals
!
EMIS_IN(237) = 'CH4_fx;CH4_12C,0.9896165;CH4_13C,0.0103835;CH4_D0,0.9995758;CH4_D1,0.0004242;CH4_fx_e48_a01',
                                                          'import_grid', 'Mfx_wa_CH4', 'GP=2', !wild animals
```

S5.5 TNUDGE

Namelist 7. Example entries to nudge the tracers `CH4` and `CH4_fx` to a predefined lower boundary condition.

```
!# SYNTAX:
!#          tracer, subname, channel, object, nudging-coeff. [s],
!#          min.lat, max.lat, min.lev, max.lev, min.lon, max.lon,
!#          flux diagnostic ?
!# NOTES:
!#   - special levels: -3 boundary layer ,-2 tropopause, -1 top, 0 surface
!#   - nudging-coeff < 0: apply 'hard' nudging with coeff = model time step
!#
! GHG
TNUDGE_GP(2)  = 'CH4','',     'import_grid','TN_GHG_CH4',10800.0,-90.0,90.0,0,0,0.0,360.0,T,'','','','',0,
!
```

```
TNUDGE_GP(4)  = 'CH4','fx',   'import_grid','TN_GHG_CH4',10800.0,-90.0,90.0,0,0,0.0,360.0,T,'','','','',0,
!
```

S5.6 H2OISO

Namelist 8. Namelist of the submodel H2OISO as used in the presented examples.

```
&CTRL
/
&CPL
l_steady = T         ! start from steady-state conditions
                     ! this means q, xl and xi are initialized by
                     ! H2OISOHHOvap, H2OISOHHOliq and H2OISOHHOice,
                     ! which are initialized via tracer.nml
l_noconvect_dd = F   ! set true only for sensitivity study
                     ! without influence of convect on deltaD
l_nocloud_dd   = F   ! set true only for sensitivity study
                     ! without influence of cloud on deltaD
/
```

References

Atkinson, R.: Kinetics of the gas-phase reactions of OH radicals with alkanes and cycloalkanes, Atmos. Chem. Phys., 3, 2233–2307, 2003.

Brass, M. and Röckmann, T.: Continuous-flow isotope ratio mass spectrometry method for carbon and hydrogen isotope measurements on atmospheric methane, Atmos. Meas. Tech., 3, 1707–1721, https://doi.org/10.5194/amt-3-1707-2010, https://www.atmos-meas-tech.net/3/1707/2010/, 2010.

Brinkop, S. and Jöckel, P.: ATTILA 4.0: Lagrangian advective and convective transport of passive tracers within the ECHAM5/MESSy (2.53.0) chemistry–climate model, Geosci. Model Dev., 12, 1991–2008, https://doi.org/10.5194/gmd-12-1991-2019, https://www.geosci-model-dev.net/12/1991/2019/, 2019.

Bruhwiler, L. M. P., Michalak, A. M., Peters, W., Baker, D. F., and Tans, P.: An improved Kalman Smoother for atmospheric inversions, Atmos. Chem. Phys., 5, 2691–2702, https://doi.org/10.5194/acp-5-2691-2005, https://www.atmos-chem-phys.net/5/2691/2005/, 2005.

Eichinger, R., Jöckel, P., Brinkop, S., Werner, M., and Lossow, S.: Simulation of the isotopic composition of stratospheric water vapour - Part 1: Description and evaluation of the EMAC model, Atmos. Chem. Phys., 15, 5537–5555, https://doi.org/10.5194/acp-15-5537-2015, 2015.

Fletcher, M., E., S., Tans, P. P., Bruhwiler, L. M., Miller, J. B., and Heimann, M.: CH_4 sources estimated from atmospheric observations of CH_4 and its $^{13}C/^{12}C$ isotopic ratios: 2. Inverse modeling of CH_4 fluxes from geographical regions, Glob. Biogeochem. Cycles, 18, 1–15, https://doi.org/10.1029/2004GB002224, 2004.

Frank, F.: Atmospheric methane and its isotopic composition in a changing climate: A modelling study, Ph.D. thesis, Ludwigs Maximillian Universität München, 2018.

Jöckel, P., Kerkweg, A., Buchholz-Dietsch, J., Tost, H., Sander, R., and Pozzer, A.: Technical Note: Coupling of chemical processes with the Modular Earth Submodel System (MESSy) submodel TRACER, Atmos. Chem. Phys., 8, 1677–1687, https://doi.org/10.5194/acp-8-1677-200, https://www.atmos-chem-phys.net/8/1677/2008/, 2008.

Kerkweg, A., Sander, R., Tost, H., and Jöckel, P.: Technical note: Implementation of prescribed (OFFLEM), calculated (ONLEM), and pseudo-emissions (TNUDGE) of chemical species in the Modular Earth Submodel System (MESSy), Atmos. Chem. Phys., 6, 3603–3609, https://doi.org/10.5194/acp-6-3603-2006, https://www.atmos-chem-phys.net/6/3603/2006/, 2006.

Kiyosu, Y.: Hydrogen isotopic compositions of hydrogen and methane from some volcanic areas in northeastern Japan, Earth and Planetary Science Letters, 62, 41–52, https://doi.org/10.1016/0012-821X(83)90069-9, 1983.

McKinney, C. R., McCrea, J. M., Epstein, S., Allen, H. A., and Urey, H. C.: Improvements in Mass Spectrometers for the Measurement of Small Differences in Isotope Abundance Ratios, The Review of Scientific Instruments, 21, 724–730, https://doi.org/10.1063/1.1745698, 1950.

Monteil, G., Houweling, S., Dlugockenky, E. J., Maenhout, G., Vaughn, B. H., White, J. W. C., and Rockmann, T.: Interpreting methane variations in the past two decades using measurements of CH_4 mixing ratio and isotopic composition, Atmos. Chem. Phys., 11, 9141–9153, 2011.

Quay, P., Stutsman, J., Wilbur, D., Snover, A., Dlugokencky, E., and Brown, T.: The isotopic composition of atmospheric methane, Glob. Biogeochem. Cycles, 13, 445–461, 1999.

Rigby, M., Manning, A. J., and Prinn, R. G.: The value of high-frequency high-precision methane isotopologue measurements for source and sink estimation, J. Geophys. Res., 117, D12 312, https://doi.org/10.1029/2011JD017384, 2012.

Röckmann, T., Brass, M., Borchers, R., and Engel, A.: The isotopic composition of methane in the stratosphere: high-altitude balloon sample measurements, Atmos. Chem. Phys., 11, 13 287–13 304, https://doi.org/10.5194/acp-11-13287-2011, 2011.

Sander, R., Baumgaertner, A., Gromov, S., Harder, H., Jöckel, P., Kerkweg, A., Kubistin, D., Regelin, E., Riede, H., Sandu, A., Taraborrelli, D., Tost, H., and Xie, Z.-Q.: The atmospheric chemistry box model CAABA/MECCA-3.0, Geosci. Model Dev., 4, 373–380, https://doi.org/10.5194/gmd-4-373-2011, 2011.

Snover, A. and Quay, P.: Hydrogen and carbon kinetic isotope effects during soil uptake of atmospheric methane and a temperate grassland, Glob. Biogeochem. Cycles, 14, 25–39, 2000.

Umezawa, T., MacHida, T., Ishijima, K., Matsueda, H., Sawa, Y., Patra, P. K., Aoki, S., and Nakazawa, T.: Carbon and hydrogen isotopic ratios of atmospheric methane in the upper troposphere over the Western Pacific, Atmos. Chem. Phys., 12, 8095–81 113, https://doi.org/10.5194/acp-12-8095-2012, 2012.

White, J., Vaughn, B., and Michel, S.: University of Colorado, Institute of Arctic and Alpine Research (INSTAAR), Stable Isotopic Composition of Atmospheric Methane (^2H) from the NOAA ESRL Carbon Cycle Cooperative Global Air Sampling Network, 2005-2009, Version: 2016-04-26, ftp://aftp.cmdl.noaa.gov/data/trace_gases/ch4h2/flask/, 2016.

White, J., Vaughn, B., and Michel, S.: University of Colorado, Institute of Arctic and Alpine Research (INSTAAR), Stable Isotopic Composition of Atmospheric Methane (^{13}C) from the NOAA ESRL Carbon Cycle Cooperative Global Air Sampling Network, 1998-2016, Version: 2018-01-31, ftp://aftp.cmdl.noaa.gov/data/trace_gases/ch4c13/flask/, 2017.

Whiticar, M. and Schaefer, H.: Constraining past global tropospheric methane budgets with carbon and hydrogen isotope ratios in ice., Philosophical transactions, Series A, 365, 1793–1828, https://doi.org/10.1098/rsta.2007.2048, 2007.

Zazzeri, G., Lowry, D., Fisher, R. E., France, J. L., Lanoisell, M., and Nisbet, E. G.: Plume mapping and isotopic characterisation of anthropogenic methane sources, Atmos. Environ., 110, 151–162, https://doi.org/10.1016/j.atmosenv.2015.03.029, 2015.